Progress In Electromagnetics Research M, Vol. 52, 89–97, 2016

Research on the Propagation of Extremely Low Frequency Electromagnetic Wave in Shallow Sea Area

Xiaodong Qu[1, 2, *], Guangyou Fang[1], and Hejun Yin[1]

Abstract—This paper analyzes the extremely low frequency electromagnetic wave excited by a horizontal electric dipole immersed in the sea. Analytical solutions in the air from HED underwater are deduced using a three-layer model. The effect of the sea-air interface is studied along two perpendicular directions. The electric field is inversely proportional to the square of r while the magnetic field is inversely proportional to the cube of r along the interface. By decomposing the total response into direct, up-going and down-going components, contributions of each component are discussed, indicating that interference cancellation effect occurs among the arrival electromagnetic signals from multi-paths at specific offsets and frequencies.

1. INTRODUCTION

Extremely low frequency (ELF) electromagnetic (EM) wave radiation and propagation underwater has attracted great attention for a long time [1], such as underwater target detection [2, 3], submarine navigation and communications [4–6], and marine controlled source electromagnetic (MCSEM) [7, 8]. In shallow sea area, EM methods are reconsidered for communications between autonomous underwater vehicles (AUV) while acoustic communication is limited by ambient interference, unlike in deep water. However, propagating in the seawater, high frequency EM wave will suffer from great loss for about 55 dB per wavelength [9]. In seawater of conductivity of 4 S/m, the EM wave at 1 Hz attenuates at 0.035 dB/m. Thus, ELF EM waves can provide attractive benefits for communication underwater, from land to underwater or from underwater to land.

The radiation from an electric dipole source has been studied in great details. Among many standout researchers, Weaver [10] derived the solutions for horizontal and vertical electric dipole (HED/VED) in a two-layer conductive medium, and the two-layer model was extended by [11–16]. Furthermore, the works in [9] and [17–19] gave the solutions on the radiation problem when the HED or VED was placed in a conducting medium or dielectric layer. Finally, Fares et al. [20] conducted experiments to verify Weaver's work. They measured the magnetic fields generated by HED and VED antennas in shallow seawater at bandwidth of 20 to 500 Hz, and the results indicated that the magnetic fields picked up by tri-axial magnetometer were consistent with Weaver's model.

The works in [19] derived complete solutions for the EM field of an HED underwater. Based on the work, we derive the analytical solutions above the air-sea surface based on a three-layer model that contains semi-infinite air, finite seawater and semi-infinite seabed. We employ fast Hankel transform algorithm to solve the infinite integrations containing Bessel functions, and all the simulation results fit for the FEKO very well. When the source is located in seawater, and the observation points are located approaching the surface, the propagation becomes complex due to the effect of multi-paths. Therefore, it is meaningful to analyze the attenuation curves along the cross-line (the direction perpendicular to the

Received 13 October 2016, Accepted 11 November 2016, Scheduled 28 November 2016

* Corresponding author: Xiaodong Qu (dongdongqu@126.com).

[1] Key Laboratory of Electromagnetic Radiation and Sensing Technology, Chinese Academy of Sciences, Beijing 100190, People's Republic of China. [2] University of Chinese Academy of Sciences, Beijing 100039, People's Republic of China.

HED) and in-line direction (the direction parallel to the HED) on the sea-air interface. By decomposing the total response into direct (Di), up-going (Up) and down-going (Do) components, the contributions from multi-paths are studied in details under different conditions.

The rest of the paper is organized as follows. In Section 2, the analytical expressions are derived both in the seawater layer and in the air layer. Section 3 shows the numerical results under different simulation conductions followed by conclusions in Section 4.

2. RESPONSE FOR HED UNDER SEAWATER

Figure 1 shows the three-layer model and the coordinate system, in which $\sigma_i (i = 1, 2, 3)$ is the conductivity of each layer. $s_i (i = 1, 2)$ is the border of adjacent layer and d_1 the depth of sea. P (red dots) represents the receiver positions. Horizontal electric dipole source (AB) is located at H below sea-air interface and h from s_2, and the moment is $p = p_0 e^{-i\omega t}$, where $p_0 = IdL/4\pi\sigma_1$ and ω is the angular frequency. The parameters are shown in the figure, and HED is parallel to x while positive z is downward. In general, the conductivity of the air is 0 ($\sigma_0 = 0$), and the thicknesses of the air and seabed layers are infinite. Typical parameters employed in the model are: $\sigma_1 = 4\,\mathrm{s/m}$, $\sigma_2 = 0.5\,\mathrm{s/md}_1 = 200\,\mathrm{m}$, $H = 60\,\mathrm{m}$. In the following simulation examples, $IdL = 1\,\mathrm{A}\cdot\mathrm{m}$ is used, that is $P_0 = \frac{1}{4\pi\sigma_1}\,\mathrm{V}\cdot\mathrm{m}^2$.

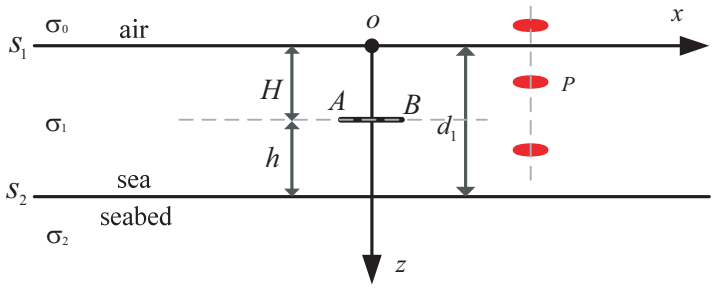

Figure 1. Model description.

Under the quasi-static condition, the expressions for the electromagnetic fields in seawater layer have been obtained in [19]. They are

$$E_{x1} = \int_0^\infty k_1^2 \left(\frac{m}{m_1} Di + Up1 + Do1\right) \cdot J_0(mr)\, dm + \int_0^\infty \left(-\frac{m}{m_1} Di + Up1 + Do1 + m_1 (Up2 - Do2)\right) \times \left(m^2 \cos^2\phi \cdot J_0(mr) + \frac{m\left(\sin^2\phi - \cos^2\phi\right)}{r} \cdot J_1(mr)\right) dm \quad (1)$$

$$E_{y1} = -\int_0^\infty \left(\frac{m}{m_1} Di + Up1 + Do1 - m_1 (Up2 - Do2)\right) \times \cos\phi \sin\phi \left(m^2 \cdot J_0(mr) - \frac{2m}{r} \cdot J_1(mr)\right) dm \quad (2)$$

$$E_{z1} = \cos\phi \int_0^\infty \left((\pm mDi - m_1 Up1 + m_1 Do1) \times m + (Up2 + Do2)\, m^3\right) \cdot J_1(mr)\, dm \quad (3)$$

$$H_{x1} = \sigma_1 \cos\phi \sin\phi \int_0^\infty m (Up2 + Do2) \times \left(mJ_0(mr) - \frac{2}{r} J_1(mr)\right) \cdot dm \quad (4)$$

$$H_{y1} = \sigma_1 \int_0^\infty (\pm mDi + m_1 (Up1 - Do1)) \cdot J_0(mr)\, dm - \sigma_1 \int_0^\infty (Up2 + Do2) \left(m^2 \cos^2\phi \cdot J_0(mr) + \frac{m\left(\sin^2\phi - \cos^2\phi\right) \cdot J_1(mr)}{r}\right) dm \quad (5)$$

$$H_{z1} = \sigma_1 \sin\phi \int_0^\infty \left[\left(\frac{m}{m_1} Di + Up1 + Do1\right) m\right] J_1(mr)\, dm \quad (6)$$

where $Di = e^{-m_1|z-H|}$, $Up1 = C_1 e^{m_1 z}$, $Up2 = B_1 e^{m_1 z}$, $Do1 = D_1 e^{-m_1 z}$ and $Do2 = E_1 e^{-m_1 z}$, $r = \sqrt{x^2+y^2}$ is the offset (horizontal distance from the receiver to the source), m the integration variable, $m_i = \sqrt{m^2 - k_i^2}$, $k_i^2 = i\sigma_i\mu\omega$, $i = 0, 1, 2$, J the Bessel function of zero or one, ϕ the angle between the offset, and x, and C_1, D_1, B_1, E_1 are Fresnel's reflection coefficients for each component and

$$C_1 = \frac{m \cdot e^{-2m_1 d_1}}{m_1} \cdot \left[\frac{N_{01} \cdot e^{-m_1 H} - e^{m_1 H}}{M_{12} - N_{01} \cdot e^{-2m_1 d_1}}\right], \quad D_1 = \frac{m}{m_1} \cdot N_{01} \cdot \left[\frac{M_{12} \cdot e^{-m_1 H} - e^{-2m_1 d_1} \cdot e^{m_1 H}}{N_{01} \cdot e^{-2m_1 d_1} - M_{12}}\right],$$

$$B_1 = \frac{e^{-2m_1 d_1}}{m} \cdot \left(\frac{e^{m_1 H} + e^{-m_1 H}}{e^{-2m_1 d_1} - T_{12}}\right) + \frac{m_1}{m^2} C_1, \quad E_1 = \frac{1}{m} \cdot \left(\frac{e^{m_1 H} \cdot e^{-2m_1 d_1} + e^{-m_1 H} \cdot T_{12}}{T_{12} - e^{-2m_1 d_1}}\right) - \frac{m_1}{m^2} D_1,$$

$$N_{01} = \frac{m_0 - m_1}{m_0 + m_1}, \quad M_{12} = \frac{1 - M}{1 + M}, \quad M = -\frac{m_1}{m_2}\frac{m_1 + m_2 \tanh(m_1 d_1)}{m_2 + m_1 \tanh(m_1 d_1)},$$

$$T_{12} = \frac{1 - T}{1 + T}, \quad T = -\frac{m_1 \sigma_2}{m_2 \sigma_1}\frac{m_1 \sigma_2 + m_2 \sigma_1 \tanh(m_1 d_1)}{m_2 \sigma_1 + m_1 \sigma_2 \tanh(m_1 d_1)}.$$

Similarly, the expressions for ELF EM wave excited by HED in the air can be obtained as follows.

$$E_{x0} = k_1^2 \int_0^\infty C_0 e^{m_0 z} J_0(mr)\, dm + \frac{\sigma_1}{i\omega\varepsilon_0} \int_0^\infty (B_0 m_0 - C_0 m)\, e^{m_0 z} \left[\cos^2\phi \frac{\partial J_1(mr)}{\partial r} + \sin^2\phi \frac{J_1(mr)}{r}\right] dm \quad (7)$$

$$E_{y0} = -\frac{\sigma_1}{i\omega\varepsilon_0} \int_0^\infty (B_0 m_0 - C_0 m)\, e^{m_0 z} \cos\phi \sin\phi \left[\frac{\partial J_1(mr)}{\partial r} + \frac{J_1(mr)}{r}\right] dm \quad (8)$$

$$E_{z0} = \cos\phi \left[k_1^2 \int_0^\infty B_0 e^{m_0 z} J_1(mr)\, dm + \frac{\sigma_1}{i\omega\varepsilon_0} \int_0^\infty \left(B_0 m_0^2 - C_0 m_0 m\right) e^{m_0 z} J_1(mr)\, dm\right] \quad (9)$$

$$H_{x0} = \sigma_1 \cos\phi \sin\phi \int_0^\infty m^2 B_0 e^{m_0 z} J_0(mr)\, dm - \sigma_1 \cos\phi \sin\phi \int_0^\infty m B_0 e^{m_0 z} \frac{2}{r} J_1(mr)\, dm \quad (10)$$

$$H_{y0} = \sigma_1 \int_0^\infty \left[\left(m_0 C_0 - m^2 \cos^2\phi B_0\right) e^{m_0 z}\right] \cdot J_0(mr) dm - \sigma_1 \int_0^\infty B_0 e^{m_0 z} \frac{m\left(\sin^2\phi - \cos^2\phi\right)}{r} J_1(mr) dm \quad (11)$$

$$H_{z0} = \sigma_1 \sin\phi \int_0^\infty C_0 e^{m_0 z} m J_1(mr)\, dm \quad (12)$$

where C_0 and B_0 are Fresnel's reflection coefficients for each component and

$$C_0 = \frac{m \cdot (1 - N_{01})}{m_1 \cdot e^{m_1 H}} \cdot \left[\frac{M_{12} - e^{-2m_1 d_1} \cdot e^{2m_1 H}}{M_{12} - N_{01} \cdot e^{-2m_1 d_1}}\right], \quad B_0 = \frac{(1 - N_{01})}{m \cdot e^{m_1 H}} \cdot \left[\frac{M_{12} - e^{-2m_1 d_1} \cdot e^{2m_1 H}}{M_{12} - N_{01} \cdot e^{-2m_1 d_1}}\right].$$

In the following section, the ELF EM field under seawater can be calculated using Eq. (1)–Eq. (6) while the field in the air can be obtained by Eq. (7)–Eq. (12). The expressions for field in the seawater are more complex than that in the air. This is because the propagation path from the source to the observe point in the air is simpler, and only the up-going EM field can be picked up.

To analyze the multi-paths, the observation point is placed in the sea water, shown in Fig. 2. There exist typically five paths for ELF EM wave from the transmitter to the receiver. L1 is called lateral

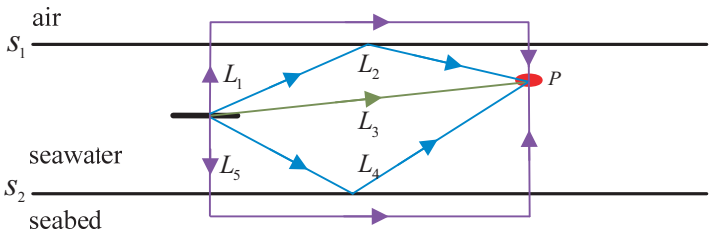

Figure 2. Propagation paths.

wave or air wave in some literature where the EM wave mainly travels in the air. L2 is the component reflected by s_1 while L4 is from the reflection of s_2. L3 is direct wave traveling from the source to the receiver directly. L5 is the part traveling along the seabed. Unlike previous works, the total response will be decomposed into three parts: direct wave, up-going wave which comes from the reflection of s_2 and down-going wave that originates from the reflection of s_1. Thus, the up-going component mainly contains L4 and L5, and the down-going part contains L1 and L2. Using E_x as an example, we have the following results:

$$E_{xDi} = \int_0^\infty \left(k_1^2 - m^2\cos^2\phi\right)\frac{m}{m_1}Di \cdot J_0(mr)\,dm + \int_0^\infty -\frac{m}{m_1}Di\frac{m\left(\sin^2\phi - \cos^2\phi\right)}{r}\cdot J_1(mr)dm \quad (13)$$

$$E_{xUp} = \int_0^\infty \left(\left(k_1^2 - m^2\cos^2\phi\right)Up1 + m_1m^2\cos^2\phi Up2\right)\cdot J_0(mr)\,dm \quad (14)$$

$$+\int_0^\infty (-Up1 + m_1Up2)\cdot\frac{m\left(\sin^2\phi - \cos^2\phi\right)}{r}\cdot J_1(mr)\,dm \quad (15)$$

$$E_{xDo} = \int_0^\infty \left(\left(k_1^2 - m^2\cos^2\phi\right)Do1 - m_1m^2\cos^2\phi Do2\right)\cdot J_0(mr)dm \quad (16)$$

$$-\int_0^\infty (Do1 + m_1Do2)\frac{m\left(\sin^2\phi - \cos^2\phi\right)}{r}\cdot J_1(mr)\,dm \quad (17)$$

where $E_{xDi}, E_{xUp}, E_{xDo}$ represent direct wave, up-going wave and down-going wave, respectively.

To evaluate contributions of decomposed components to the total response, the percentage of the total field for each component is defined as follows:

$$P_{Ei} = \frac{|E_i|}{|E|}\times 100 \quad (i = Di, Do, Up) \quad (18)$$

And, the total percentage is

$$PE_{tot} = \sum PE_i = \frac{|E_{Di}|}{|E|} + \frac{|E_{Do}|}{|E|} + \frac{|E_{Up}|}{|E|} = \frac{|E_{Di}| + |E_{Do}| + |E_{Up}|}{|E_{Di} + E_{Do} + E_{Up}|} \geq 100 \quad (19)$$

In the following section, the three contributors are evaluated using Eq. (16), and the total response is calculated using Eq. (17). The total percentage is larger than 100%, which shows that interference cancelation effect exists between the components from multi-paths.

3. NUMERICAL RESULTS

3.1. The Effect of the Sea-Air Interface

Having deduced the solutions for the ELF EM fields excited by HED immersed in sea, the effect of the sea-air interface (boundary s_1) can be studied along two perpendicular directions (in-line and cross-line direction relative to the source). Fig. 3 shows the attenuation curves for the EM field in the seawater and Fig. 4 in the air, in which (a) and (b) show how the electric and magnetic fields change with the offset in cross-line direction respectively while (c) and (d) show the relations in in-line direction. The operation frequency is 2 Hz, and the observation points are 0.1 m above or below s_1.

Along the cross-line direction, the electric field contains only x component, and the electric fields of both sides are equal. The magnetic field contains y and z components and is continuous across the sea-air interface. The y component dominates the whole response, especially in far region. Magnetic fields are mainly generated by the current, which form two opposite magnetic dipoles around the HED due to the good conductivity of the sea. Thus, the magnetic field is almost inversely proportional to the square of r firstly when the offset is less than 300 m, and cube of r eventually when the offset is more than 600 m.

Along the in-line direction, the magnetic field contains only y component which is continuous across the boundary and is inversely proportional to the square of r at offset less than 300 m and cube of r at offset more than 600 m. However, above s_1, electric field contains x component and z component

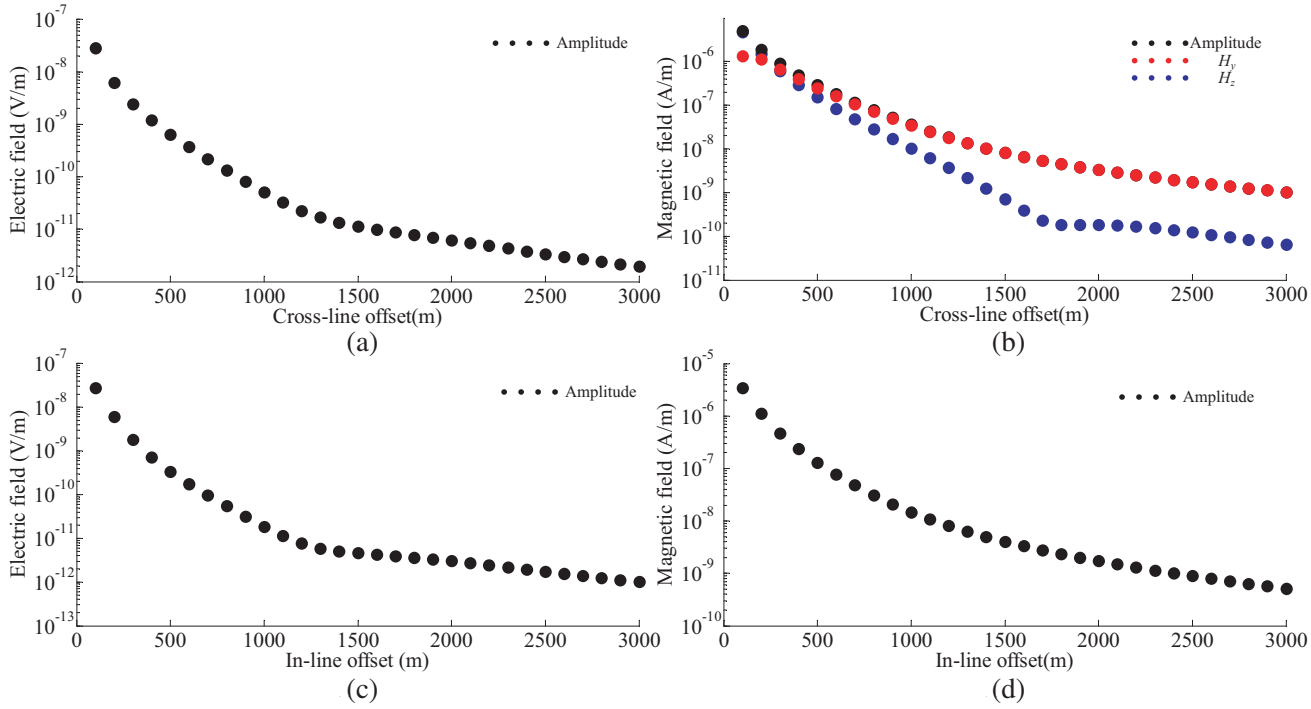

Figure 3. The attenuation curves for electric and magnetic field below the sea-air interface: (a) (b) cross-line direction; (c) (d) in-line direction.

while only x component exists under s_1 which shows that electric field undersea will be parallel to the sea-air boundary eventually. Furthermore, the surface charges are induced upon the surface, which contribute to the electric field in the air. Therefore, along the in-line direction, the electric field is inversely proportional to the square of r.

3.2. Contributions for the Decomposed Components

Figure 5 shows the contributions of each component and the total percentage along the in-line direction when the observation point is at different offsets (100 m ∼ 3000 m) and depths (0 ∼ 120 m) when the operation frequency is 2 Hz.

It is clear that direct wave dominates the total response at small offsets while up-going and down-going waves account for a smaller proportion. As the offset increasing, up-going and down-going components begin to occupy a larger proportion. When the offset is 1000 ∼ 2000 m, the percentages of up-going and down-going components are more than 100%, indicating that interference cancelation effect between the two components occurs and reduces the total amplitude. At large offset, the down-going wave dominates the total response for the reason that the wave travels at a smaller attenuation rate via L1 path (air wave or lateral wave). The total percentage shown in Fig. 5(d) indicates the interference cancelation effect among the arrival fields from multi-paths at different offsets and vertical depths. The red color stands for the greatest interference effect. Thus, the attenuation curve of the electric field under s_1 appears inflection point at the offset of 1000 ∼ 2000 m in Fig. 3 and Fig. 4. On the other hand, we can find that the up-going wave mainly exists at the offset of 1000 ∼ 2000 m where the down-going wave exists as well. Therefore, it is difficult to separate the underground information in shallow sea area from the down-going wave (mainly air wave) and measures must be taken to remove the air wave in marine controlled source electromagnetic method (MCSEM).

Figure 6 shows the contributions represented in percentage of each component along the in-line direction under different operation frequencies (1 Hz ∼ 20 Hz) and vertical depths (0 ∼ 120 m) at a specific offset (1000 m). At this particular offset, the direct wave possesses a small percentage while the total response is dominated by the down-going parts at all frequencies and depths in the sea.

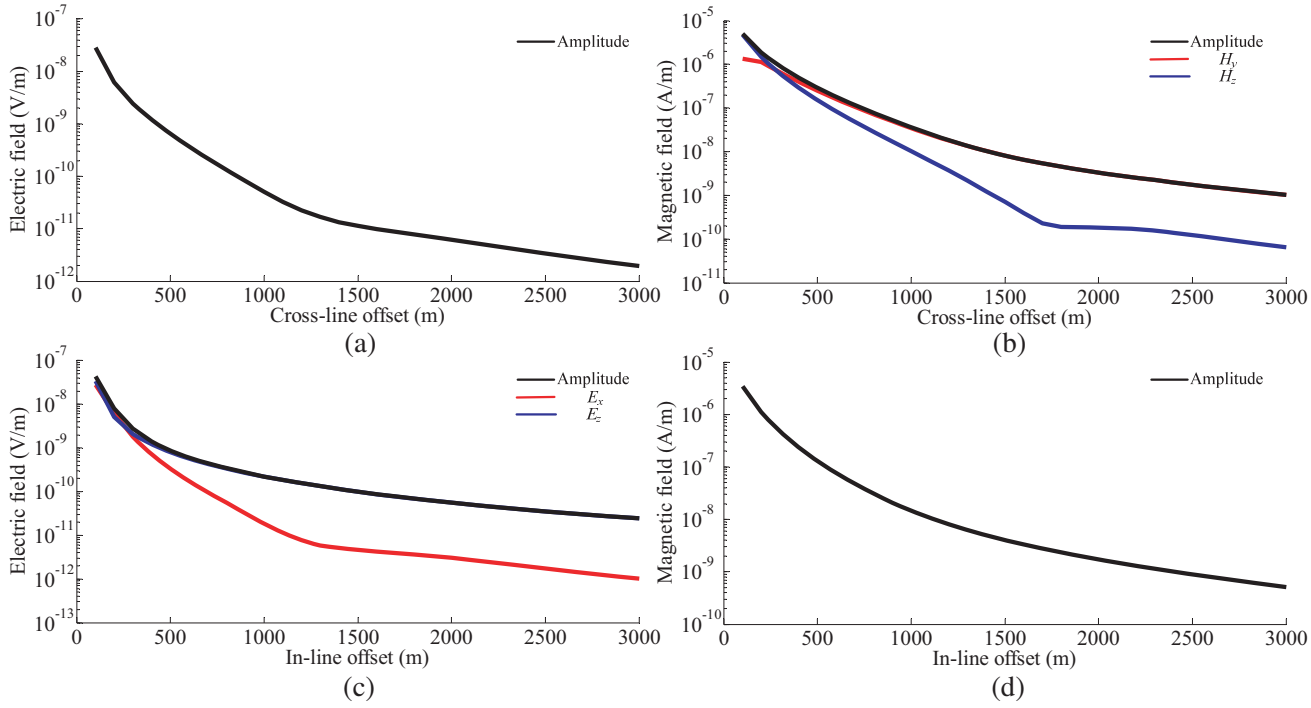

Figure 4. The attenuation curves for electric and magnetic field above the sea-air interface: (a) (b) cross-line direction; (c) (d) in-line direction.

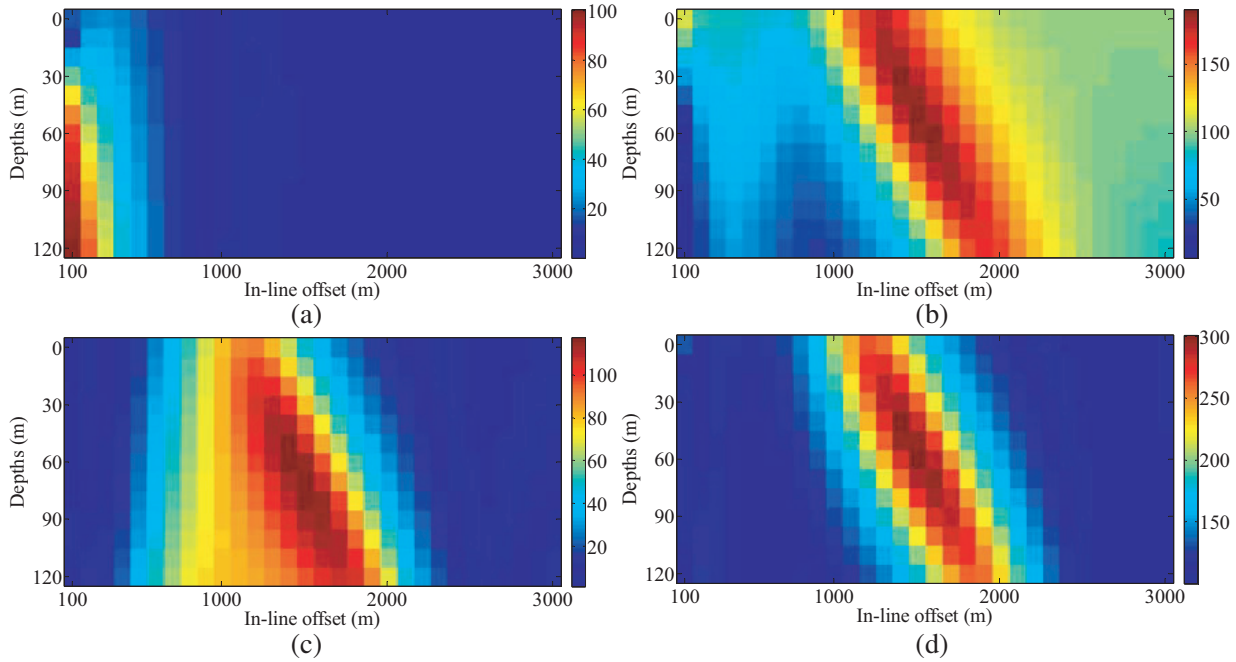

Figure 5. The contributions of each component at frequency of 2Hz expressed as a percentage (%): (a) Di; (b) Do; (c) Up; (d) the total percentage.

Furthermore, the up-going wave affects the total response at low frequencies and deep depths where the observation point approaches the boundary s_2. Also, Fig. 6(d) shows the interference cancelation effect clearly at low frequencies.

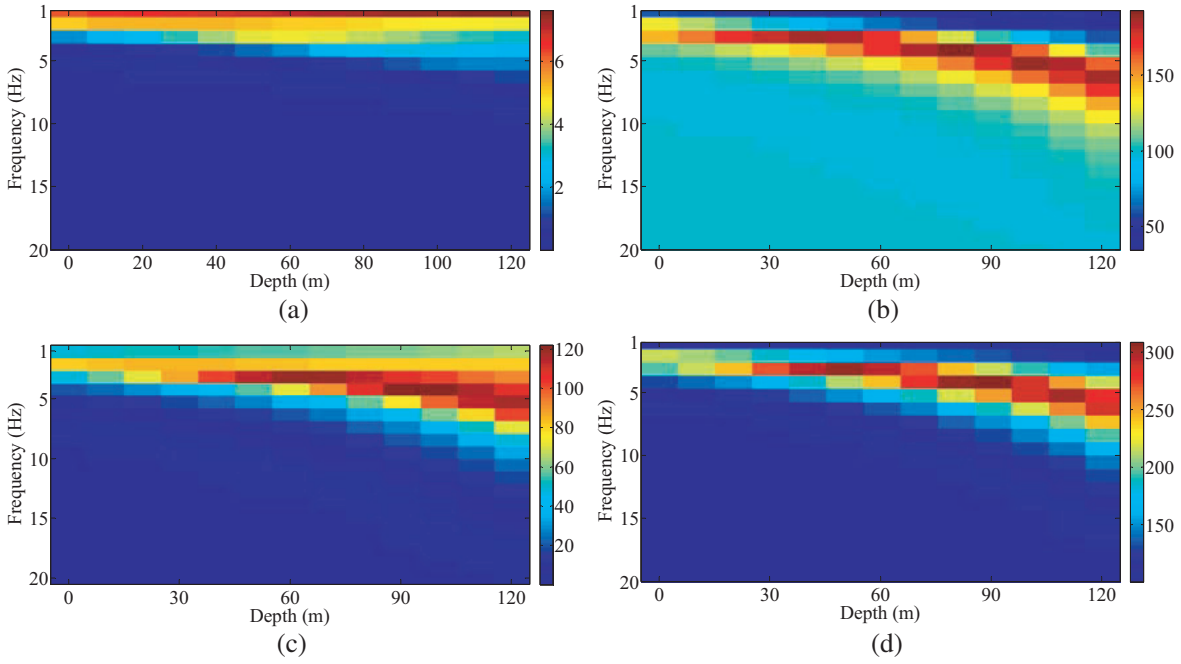

Figure 6. The contributions of each component at offset of 1000m expressed as a percentage (%): (a) Di; (b) Do; (c) Up; (d) the total percentage.

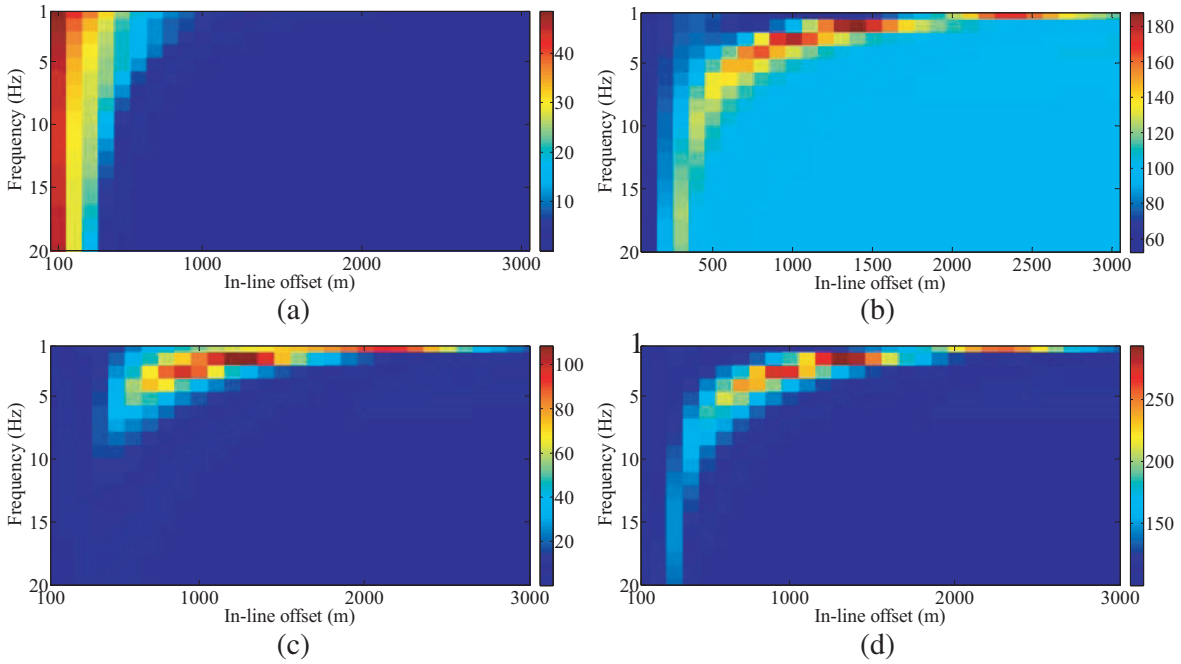

Figure 7. The contributions of each component at depth of 30m expressed as a percentage (%): (a) Di; (b) Do; (c) Up; (d) the total percentage.

Figure 7 shows the contributions of each component and the total percentage along the in-line direction with different operation frequencies ($1\,Hz \sim 20\,Hz$) and offsets ($100\,\mathrm{m} \sim 3000\,\mathrm{m}$) at a specific vertical depth ($30\,\mathrm{m}$). The direct component dominates the response at small offset while the down-going part contributes more than 90% at large offsets and high frequencies. However, at low frequencies

and small offsets, the up-going wave affects the response as well as down-going part. Thus, interference cancelation effect shown in Fig. 7(d) occurs at low frequencies and small offsets.

4. CONCLUSION

In this paper, we derive analytical solutions in the air for HED undersea based on previous work. The simulation results show that the sea-air interface has an important effect on the propagation of ELF electromagnetic fields. Firstly, the electric field is inversely proportional to the square of r while the magnetic field is inversely proportional to the cube of r along the interface. Secondly, the down-going component dominates the total response almost at all frequencies and offsets due to the multi-path effect. Thirdly, interference cancelation effect occurs at some specific offsets, and the most distinct feature is the inflection points on the attenuation curves. These conclusions may provide useful references in three aspects as follows: arrange sensor arrays in a reasonable way in underwater target detection; optimize transceiver and receiver antennas and positions for different occasions in magnetic communications; develop time domain or frequency domain methods to remove the airwave in shallow MSCEM.

REFERENCES

1. Wait, J. R., *Electromagnetic Wave in Stratified Media*, Pergamon, New York, 1970.
2. Schaefer, D., J. Doose, M. Pichlmaier, et al., "Conversion of UEP signatures between different environmental conditions using shaft currents," *IEEE Journal of Oceanic Engineering*, Vol. 41, No. 1, 105–111, Mar. 2015.
3. Yaakobi, O., G. Zilman, and T. Miloh, "Detection of the electromagnetic field induced by the wake of a ship moving in a moderate sea state of finite depth," *Journal of Engineering Mathematics*, Vol. 70, No. 1, 17–27, Jul. 2011.
4. Bui, V. P. and W. S. Yeoh, "Propagation and channel characteristics in seawater environment," *IEEE Antennas and Propagation Society International Symposium*, 701–702, Jul. 2014.
5. Bush, B. F., V. K. Tripp, and K. Naishadham, "Practical modeling of radio wave propagation in shallow seawater," *Proceedings of the 2012 IEEE International Symposium on Antennas and Propagation*, 1–2, Jul. 2012.
6. Arutaki, A. and J. Chiba, "Communication in a three-layered conducting media with a vertical magnetic dipole," *IEEE Transactions on Antennas & Propagation*, Vol. 28, No. 4, 551–556, Jul. 1980.
7. Chen, J. and D. L. Alumbaugh, "Three methods for mitigating airwaves in shallow water marine controlled-source electromagnetic data," *Geophysics*, Vol. 76, No. 2, 4542–4544, May 2011.
8. Amundsen, L., L. Løseth, R. Mittet, et al., "Decomposition of electromagnetic fields into upgoing and downgoing components," *Geophysics*, Vol. 71, No. 5, 211–223, Sep. 2006.
9. Liu, C., L. G. Zheng, and Y. P. Li, "Study of ELF electromagnetic fields from a submerged horizontal electric dipole positioned in a sea of finite depth," *IEEE International Symposium on Microwave, Antenna, Propagation and EMC Technologies for Wireless Communications*, 2009.
10. Weaver, J. T., "The quasi-static field of an electric dipole embedded in a two-layer conducting half-space," *Canadian Journal of Physics*, Vol. 45, No. 6, 1981–2002, Jan. 1967.
11. King, R. W. P., "The electromagnetic field of a horizontal electric dipole in the presence of a three-layered region," *J. Appl. Phys.*, Vol. 69, No. 12, 7987–7995, 1991.
12. King, R. W. P., "The electromagnetic field of a horizontal electric dipolein the presence of a three-layered region: Supplement," *J. Appl. Phys.*, Vol. 74, No. 8, 4845–4548, 1993.
13. Liu, L. and K. Li, "Radiation from a vertical electric dipole in the presence of a three-layered region," *IEEE Transactions on Antennas & Propagation*, Vol. 55, No. 12, 3469–3475, 2007.
14. Li, K. and Y. Lu, "Electromagnetic field generated by a horizontal electric dipole near the surface of a planar perfect conductor coated with a uniaxial layer," *IEEE Transactions on Antennas & Propagation*, Vol. 53, No. 10, 3191–3200, 2005.

15. Xu, Y. H., K. Li, and L. Liu, "Electromagnetic field of a horizontal electric dipole in the presence of a four-layered region," *Progress In Electromagnetics Research*, Vol. 81, 371–391, 2008.
16. Zhi, Y. J., K. Li, and Y. T. Fang, "Electromagnetic field of a horizontal infinitely long wire over the dielectric-coated earth," *IEEE Transactions on Antennas & Propagation*, Vol. 60, No. 1, 360–366, 2012.
17. Zhang, H. Q., W. Y. Pan, K. Li, et al., "Electromagnetic field for a horizontal electric dipole buried inside a dielectric layer coated high loss half space," *Progress In Electromagnetics Research*, Vol. 50, 163–186, 2005.
18. Liu, L., K. Li, and W. Y. Pan, "Electromagnetic field from a vertical electric dipole in a four-layered region," *Progress In Electromagnetics Research B*, Vol. 8, 213–241, 2008.
19. Zhang, J. G., Y. Z. Qi, et al., "Research on 3D marine electromagnetic interferometry with synthetic sources for suppressing the airwave interference," *Applied Geophysics*, Vol. 10, No. 4, 373–383, 2013.
20. Fares, S. A., R. Fleming, D. Dinn, et al., "Horizontal and vertical electric dipoles in a two-layer conducting medium," *IEEE Transactions on Antennas & Propagation*, Vol. 62, No. 11, 5656–5665, Nov. 2014.